



Article

Competitive Adsorption of Ionic Liquids Versus Friction Modifier and Anti-Wear Additive at Solid/Lubricant Interface—Speciation with Vibrational Sum Frequency Generation Spectroscopy

Dien Ngo ^{1,†}, Xin He ², Huimin Luo ³, Jun Qu ² and Seong H. Kim ^{1,*}

¹ Department of Chemical Engineering and Materials Research Institute, Pennsylvania State University, University Park, PA 16802, USA; dienngothe@gmail.com

² Materials Science and Technology Division, Oak Ridge National Laboratory, Oak Ridge, TN 37831, USA; hex1@ornl.gov (X.H.); qujn@ornl.gov (J.Q.)

³ Energy and Transportation Science Division, Oak Ridge National Laboratory, Oak Ridge, TN 37831, USA; luoh@ornl.gov

* Correspondence: shkim@engr.psu.edu or shk10@psu.edu

† Current address: Avery Dennison, 8080 Norton Parkway, Mentor, OH 44060, USA.

Received: 12 October 2020; Accepted: 10 November 2020; Published: 12 November 2020



Abstract: A modern lubricant contains various additives with different functionalities and the interactions or reactions between these additives could induce synergistic or antagonistic effects in tribological performance. In this study, sum frequency generation (SFG) spectroscopy was used to investigate competitive adsorption of lubricant additives at a solid/base oil interface. A silica substrate was used as a model solid surface. The lubricant additives studied here included two oil-soluble ionic liquids (ILs, [N888H][DEHP] and [P8888][DEHP]), an antiwear additive (secondary ZDDP), an organic friction modifier (OFM), and a dispersant (PIBSI). Our results showed that for mixtures of ZDDP and IL in a base oil (PAO4), the silica surface is dominated by the IL molecules. In the cases of base oils containing OFM and IL, the silica/lubricant interface is dominated by OFM over [N888H][DEHP], while it is preferentially occupied by [P8888][DEHP] over OFM. The presence of PIBSI in the mixture of PAO4 and IL leads to the formation of a mixed surface layer at the silica surface with PIBSI as a major component. The SFG results in this investigation provide fundamental insights that are helpful to design the formulation of new lubricant additives of desired properties.

Keywords: ionic liquids; lubricants; sum frequency generation spectroscopy; base oil; additives

1. Introduction

Lubrication plays an important role in reliable performance and durability of many engine systems and machineries [1–3]. In practice, commercial lubricants consist of various components with different functionalities such as a base oil, friction modifier, antiwear additive, antioxidant, antifoam, and detergent [4]. The presence of multiple additives in the lubricant can improve the lubrication efficiency (lower friction and wear prevention), but it can also induce unwanted antagonistic effects as reported in some tribological studies [5–10]. When a secondary zinc dialkyldithiophosphate (sec-ZDDP) was added to a lubricant mixture consisting of polyalphaolefin (PAO4) base oil, molybdenum dithiocarbamate (MoDTC), and polyisobutylene succinimide (PIBSI), for example, the friction coefficient and wear of a cast iron were reported to be higher than those in the case without adding sec-ZDDP [10]. Such reduced performances could be due to the reaction or interaction between sec-ZDDP and PIBSI in the mixed liquid. It is, therefore, important to understand chemical interactions between potential

additives to predict or design lubricant formulations for specific applications. The adsorption of a compound (base oil or additive) to a solid surface can be affected by other components in lubricants [11] and compositional or structural information of molecular layers at the interface between a solid and a mixed liquid (lubricant) is needed to understand the tribological performance of a lubricant.

Oil-soluble ionic liquids (ILs) have recently been developed as a new class of friction-reducing and wear-protecting lubricant additives [12] and compatibilities of some ILs with other lubricant additives have been reported lately [6,9,10]. Specifically, phosphonium-phosphate ILs demonstrated synergistic effects with ZDDP [6] but did not work well when mixed with some other additives such as organic friction modifier (OFM) [9]. In contrast, an ammonium-phosphate IL worked well with OFM [9] to deliver much reduced friction and wear.

In our previous study, the competitive adsorption of a base lubricant oil (PAO4) and two oil-soluble ILs, tetraoctylphosphonium bis(2-ethylhexyl)phosphate ($[P_{888}][DEHP]$) and trioctylammonium bis(2-ethylhexyl)phosphate ($[N_{888}H][DEHP]$), at a solid surface (silica) was investigated using vibrational sum frequency generation (SFG) spectroscopy [11]. Being a surface spectroscopic technique [13–15], SFG spectroscopy has provided valuable insights into the adsorption behavior of those compounds at the solid surface. Results in the previous study showed that ILs form well-ordered layers at the silica/IL interface and they replace PAO4 at the silica surface when added to the base oil. In practice, ILs would be combined with other additives in lubricants and it is necessary to understand the structure of an adsorbed layer at the solid/lubricant interface when several additives are used together. SFG spectroscopy can differentiate characteristic vibrational bands of specific molecules at the solid/liquid interface [11,14,16–18], thus it can determine the chemical identity or structure of interfacial molecules present at the solid/liquid interface.

In the current study, SFG spectroscopy was further used to investigate surface behavior of real lubricants at the solid surface. This is the first time that adsorption behavior of real lubricants was studied by a surface specific technique. The lubricants consisted of PAO base oil and various additives including ILs, OFM, PIBSI, and ZDDP. The study used silica windows as a model solid substrate because they are optically transparent in the frequency region measured in SFG experiments, enabling access to the buried interface from the solid phase. Our results showed that most additives preferentially adsorb to the silica surface from the liquid mixtures containing one additive to the base oil. For mixtures containing IL and sec-ZDDP, IL was found to dominantly adsorb at the solid/liquid interface. The lubricants containing IL and OFM showed the preferential adsorption of $[P_{888}][DEHP]$ to the silica surface from (PAO4 + OFM + $[P_{888}][DEHP]$) mixture, but the dominance of OFM at the surface in the case of (PAO4 + OFM + $[N_{888}H][DEHP]$) mixture. When PIBSI was used along with IL in PAO4, the interfacial layer appeared to contain more PIBSI than IL. The SFG results in this study, when combined with results from tribological experiments, would provide valuable information on the tribological performance of various lubricants.

2. Materials and Methods

2.1. Materials

The two oil-soluble ionic liquids (IL), $[P_{888}][DEHP]$ and $[N_{888}H][DEHP]$, were synthesized following the protocols published previously [19,20]. The PAO4 base oil, OFM, and PIBSI were provided by ExxonMobil (Paulsboro, NJ, USA). Sec-ZDDP was obtained from Lubrizol (Wickliffe, OH, USA) and it contained ~5–10 wt.% mineral oil for flowability [10]. The chemical structures of these compounds are displayed in Figure 1. The compositions of mixed liquid samples used in the study are given in Table 1. Note that the total amount of antiwear molecules (ILs and/or ZDDP) was the same in any given fluid. The OFM was used at 0.8 wt.%, which is a typical concentration used in engine oils. The concentration of PIBSI was 2 wt.%, similar to that used to provide sufficient suspension of MoDTC in a base oil. The solid substrates used in the study were IR-grade fused silica windows (diameter = 25.4 mm;

thickness = 3.0 mm) and they were obtained from Esco Optics, Inc. (Jefferson, NJ, USA). The windows, SFG liquid cell, and glassware were cleaned following the procedure described in Ref. [11].

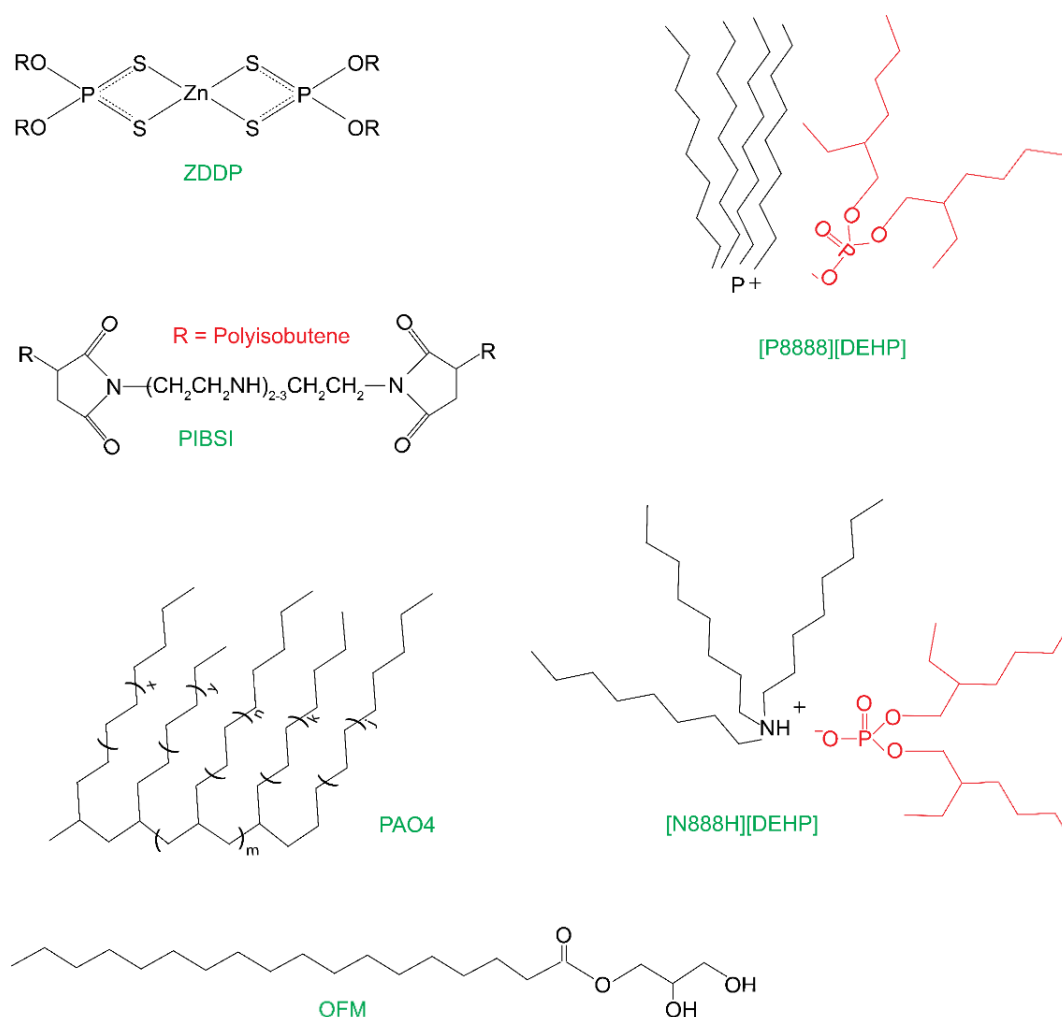


Figure 1. Chemical structures of PAO4, OFM, ZDDP, PIBSI, [N888H][DEHP], and [P8888][DEHP] used in the study. The chemical structure of OFM was not exactly known and the one shown here was suggested by NMR and Infrared spectroscopy [9]. The structure of PAO4 is a generic one [11,21].

Table 1. Chemical compositions of mixed liquid samples used in the study. The weight percent ratios were chosen so that ZDDP and ionic liquids (ILs) have the same molecular concentration in the base oil [10]. The 0.8 wt.% concentration of the organic friction modifier (OFM) is the common value used in engine oils.

Sample	Weight Percent Ratio
PAO4 + [N888H][DEHP]	99.13:0.87
PAO4 + [P8888][DEHP]	98.96:1.04
PAO4 + OFM	99.20:0.80
PAO4 + PIBSI	98.00:2.00
PAO4 + sec-ZDDP	99.20:0.80
PAO4 + OFM + [N888H][DEHP]	98.33:0.80:0.87
PAO4 + OFM + [P8888][DEHP]	98.16:0.80:1.04
PAO4 + PIBSI + [N888H][DEHP]	97.13:2.00:0.87
PAO4 + PIBSI + [P8888][DEHP]	96.96:2.00:1.04
PAO4 + sec-ZDDP + [N888H][DEHP]	99.16:0.40:0.44
PAO4 + sec-ZDDP + [P8888][DEHP]	99.08:0.40:0.52

2.2. Attenuated Total Reflectance Infrared (ATR-IR) Spectroscopy

A Bruker Vertex 80 FT-IR spectrometer equipped with a single reflection ATR accessory (Harrick MVP-Pro, Harrick Scientific Products Inc., Pleasantville, NY, USA) and a diamond crystal was used to acquire the infrared spectra of base oil and additives investigated in the current study. The spectrometer was used with an MCT detector, and each spectrum was an average of 100 scans. The spectral range was 400–4000 cm^{-1} and a spectral resolution of 4 cm^{-1} was applied. The incident angle of unpolarized IR beam at the diamond crystal/liquid interface was 45°, and a spectrum of crystal/air interface was used as the reference.

2.3. Sum Frequency Generation (SFG) Spectroscopy

A scanning pico-second sum frequency generation spectrometer (EKSPLA, Vilnius, Lithuania) was used for SFG measurements of the silica/liquid interface. The experimental geometry and liquid cell were described in details in Ref. [11]. The liquid sample was added to the sample cell and the silica window was then placed on top of the liquid. The SFG spectrometer has a tunable infrared (IR) laser from an optical parametric generator and amplifier and a visible (532 nm, Vis) laser from the pico-second laser (~27 ps, 10 Hz). The SFG beam ($\omega_{SFG} = \omega_{Vis} + \omega_{IR}$) was generated by overlapping the visible and IR laser beams spatially and temporally at the silica/liquid interface. Both *SSP* and *PPP* polarization combinations were used in SFG experiments. An *SSP* polarization combination means, for example, *S*-polarized SFG, *S*-polarized 532 nm, *P*-polarized IR with respect to the laser incident plane (Figure 2). More details of the SFG setup, spectral collection, and data processing can be found in Ref. [11].

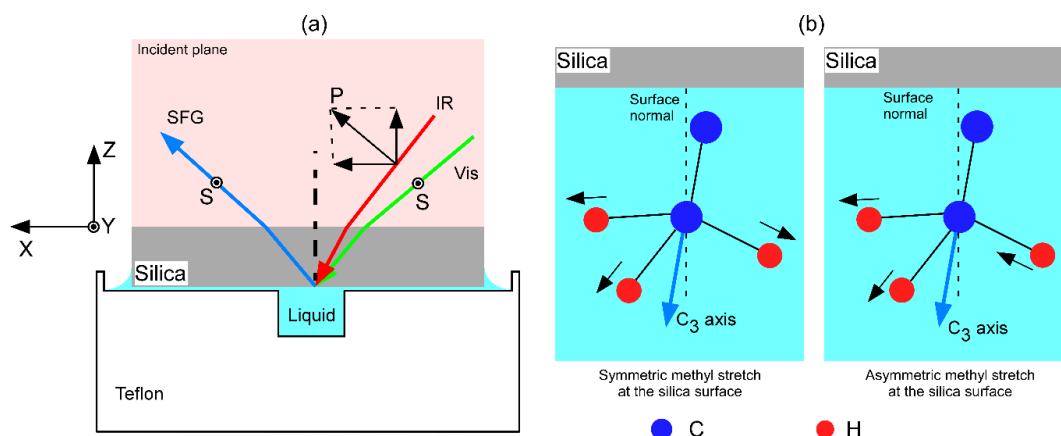


Figure 2. (a) Illustration of liquid sample cell and experimental geometry used in SFG experiments of the silica/liquid interface. The lab coordinate is the XYZ Cartesian coordinates and the incident plane of the laser beams is (XZ) plane. The symbol *S* indicates that the polarized light has its electric field vector aligned along the Y direction (perpendicular to the (XZ) plane). When the electric field vector of the polarized light is in the incident plane, it is denoted as *P*, and it has vector components aligned along X and Z directions. Figure (a) is adapted with permission from Ref. [11], Copyright © 2020 American Chemical Society. (b) Illustration of symmetric and asymmetric stretch modes of a methyl group at the silica surface.

The use of different polarization combinations helps understand the structure of the adsorbed layer at the silica surface. At the liquid/amorphous solid interface, the X and Y directions (parallel to the surface) are identical; in this case, the *SSP* polarization combination preferentially detects a transition dipole moment along the Z direction (normal to the surface, Figure 2a), while the *PPP* combination measures both surface-parallel and perpendicular components of the transition dipole moment (Figure 2a) [13]. Using different polarization combinations can, therefore, give information on the orientation of functional groups as well as the packing of the surface layer [13]. The methyl

group in Figure 2b, for example, has its symmetric axis very close to the surface normal. In this case, the relative SFG intensity of the symmetric methyl stretch mode is strong in *SSP* but weak in *PPP* measurements because its transition dipole moment is very close to the surface normal (*Z* direction). On the contrary, the transition dipole moment of the asymmetric methyl stretch mode (Figure 2b) is nearly parallel to the surface and the relative SFG intensity of this vibrational mode is strong in *PPP* but very weak in *SSP* measurements.

3. Results and Discussion

3.1. ATR-IR Spectra

The chemical structures of PAO4, sec-ZDDP, OFM, and PIBSI are not precisely known in this study, and infrared spectroscopy was used to obtain the spectra of main IR active vibrational modes in these compounds. The results from IR spectroscopy are useful for interpreting SFG spectra of base oil, additives as well as their mixtures at silica/liquid interface. The ATR-IR spectra of individual compounds used in this study are given in Figure 3.

Figure 3 shows that PAO4, OFM, and ILs have very strong peaks of symmetric methylene stretch mode ($\sim 2852\text{ cm}^{-1}$, $\text{CH}_{2,s}, d^+$) and asymmetric methylene stretch mode ($\sim 2920\text{ cm}^{-1}$, $\text{CH}_{2,as}, d^-$) [22–28]. The symmetric methyl stretch mode ($\text{CH}_{3,s}, r^+$) and the asymmetric methyl stretch mode ($\text{CH}_{3,as}, r^-$) are at $\sim 2872\text{ cm}^{-1}$ (weak) and $\sim 2956\text{ cm}^{-1}$ (medium), respectively [25–28]. The band centered at $\sim 2920\text{ cm}^{-1}$ consists of symmetric methylene Fermi resonance ($\sim 2907\text{ cm}^{-1}$, $\text{CH}_{2,s,FR}, d^+_{FR}$) and symmetric methyl Fermi resonance ($\sim 2934\text{ cm}^{-1}$, $\text{CH}_{3,s,FR}, r^+_{FR}$) [24]. Based on the works of Wang et al., the peak at $\sim 2920\text{ cm}^{-1}$ could also be attributed to the Fermi resonance between the symmetric methylene stretch and the CH_2 bending overtone [29,30]. Although the methyl group has a larger IR cross-section than the methylene group, its intensity is weaker due to a lower density in the molecule. For example, [N888H][DEHP] has 31 CH_2 groups and 7 CH_3 groups in each molecule. The IR spectra of PIBSI and sec-ZDDP are quite similar to each other and are very different from the spectra of other compounds in this study. They both have a shoulder at $\sim 2975\text{ cm}^{-1}$ that could be attributed to out-of-plane asymmetric methyl stretch [31], and the intensities of CH_2 and CH_3 stretches are comparable. Table 2 lists the typical assignments of vibrational modes of CH_2 and CH_3 in organic compounds.

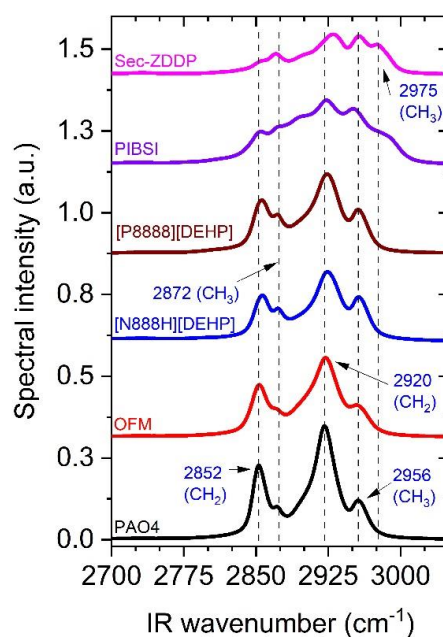


Figure 3. ATR-IR spectra of compounds used in the study. The spectra of PAO4, [N888H][DEHP], and [P8888][DEHP] are adapted from Ref. [11].

Table 2. Typical assignments of CH₂ and CH₃ groups in organic compounds. Due to the positive charge on the phosphorus atom of [P8888], P-CH₂-C is listed in the same group with N-CH₂-C and O-CH₂-C groups.

Functional Group	Frequency (cm ⁻¹)	Vibrational Mode
C-CH ₂ -C [22,25,27,28,31-33]	2845–2858	CH _{2,s} (<i>d</i> ⁺), symmetric methylene stretch
	2896–2930	CH _{2,as} (<i>d</i> ⁻), asymmetric methylene stretch
	2890–2927	CH _{2,s,FR} (<i>d</i> ⁺ _{FR}), symmetric methylene Fermi resonance
C-CH ₃ [22,25-28,31-34]	2869–2925	CH _{3,s} (<i>r</i> ⁺), symmetric methyl stretch
	2948–2973	CH _{3,as} (<i>r</i> ⁻), asymmetric methyl stretch
	2884–2942	CH _{3,s,FR} (<i>r</i> ⁺ _{FR}), symmetric methyl Fermi resonance
O-CH ₂ -C, N-CH ₂ -C, P-CH ₂ -C [29,35-37]	2870–2875	CH _{2,s} (<i>d</i> ⁺), symmetric methylene stretch
	2900	CH _{2,as} (<i>d</i> ⁻), asymmetric methylene stretch
	2938–2954	CH _{2,s,FR} (<i>d</i> ⁺ _{FR}), symmetric methylene Fermi resonance

3.2. SFG Spectra of Individual Compounds at Silica/Liquid Interface

The SFG spectra of individual compounds at the silica/liquid interface are given in Figure 4 for both *SSP* and *PPP* polarization combinations. The low signal to noise (S/N) ratios of *PPP* spectra compared to those of *SSP* spectra are due to the low reflectivity of *P*-polarized light under the experimental conditions used in the current study. The SFG spectra of PAO4, [N888H][DEHP], and [P8888][DEHP] are adapted from Ref. [11] and are given in Figure 4 for comparison as well as to support the spectral interpretation of the adsorption data of mixed compounds at the silica/liquid interface presented in other sections. Note that due to the unknown structures of some proprietary additives (esp. *sec*-ZDDP), comprehensive assignments of spectral features were quite limited for those compounds and their mixtures. The *SSP* and *PPP* spectra of silica/PIBSI could not be obtained with a reasonably good S/N ratio because their signals were so weak; this could be due to the extremely high viscosity of PIBSI, so the adsorption-driven interfacial packing was difficult. Without non-centrosymmetric order of molecules, SFG signal is extremely weak. The silica surface is different from oxide surfaces of engineering metal substrates and thus structures of adsorbed layers at these surfaces could be somewhat different. However, the SFG results in this study can still be used as reference for understanding surface behavior of lubricant base oil and additives at the metal oxide/liquid interface [11,38–41].

The *SSP* spectrum of PAO4 at the silica surface shows a medium intensity peak at ~2875 cm⁻¹ (CH_{3,s}) and a strong peak at ~2940 cm⁻¹ (CH_{3,s,FR}), while the *PPP* spectrum reveals a dominance of SFG signal from the asymmetric methyl stretch mode at ~2960 cm⁻¹ which is not observed in the *SSP* spectrum. This means that the symmetry axis of methyl groups of the PAO4 side chains is relatively perpendicular to the surface (Figure 2b). The signal of symmetric methylene stretch mode (~2850 cm⁻¹) is strong in *SSP* measurement but weak in *PPP* measurement, indicating that the alkyl chains of PAO4 align along the surface normal with gauche defects (Figure 5a) [11,13]. The segregation of the chain end to the solid surface with no specific chemical interactions provides the minimization loss of conformational entropy at the interface [42,43]. Both *SSP* and *PPP* spectra of [N888H][DEHP] and [P8888][DEHP] show three peaks at ~2850 cm⁻¹, 2870 cm⁻¹, and 2940 cm⁻¹, and the previous study has shown that the charged head groups of these IL molecules are preferentially interacting with the silica surface while their alkyl chains facing the bulk liquid (Figure 5b) [11,43].

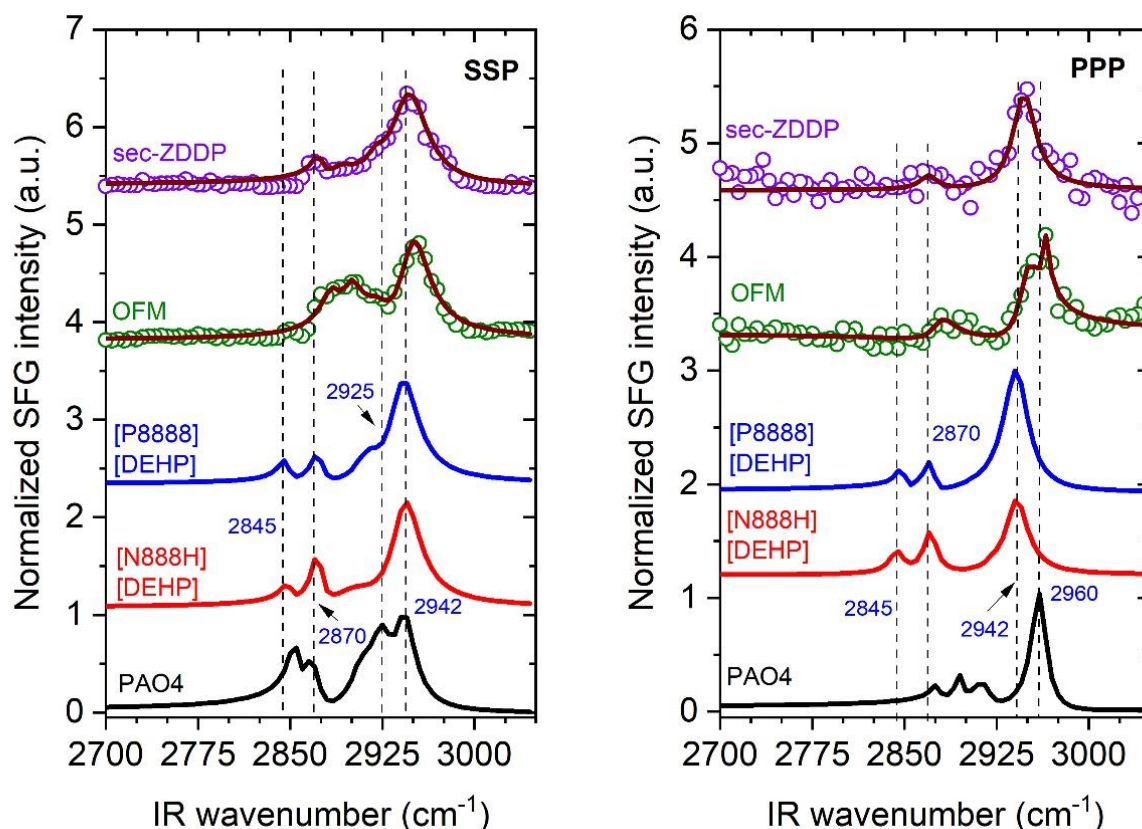


Figure 4. Sum frequency generation (SFG) spectra of single compounds at the silica/liquid interface. The solid lines are fitted curves and the fitting results are given in the SI. The line spectra of PAO4, [N888H][DEHP], and [P8888][DEHP] are adapted from Ref. [11] and are shown here for comparison.

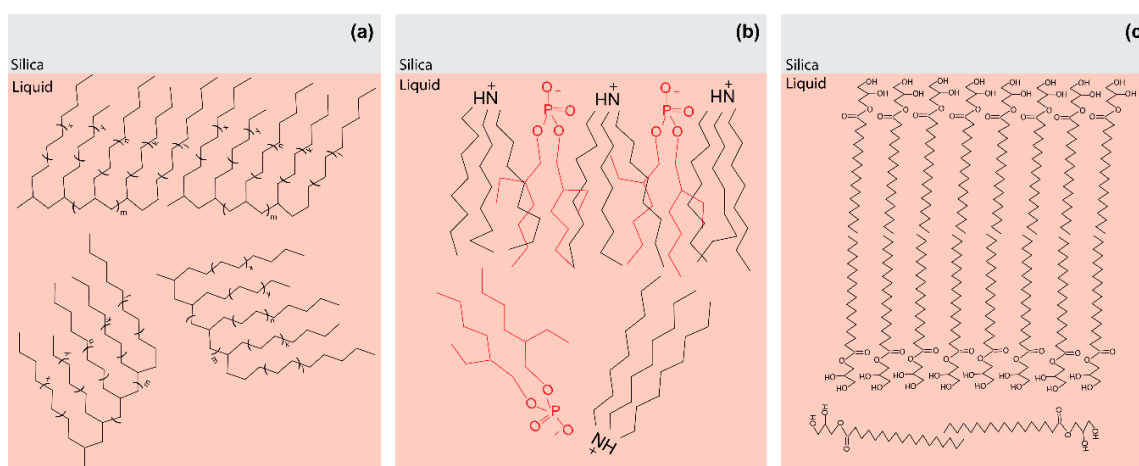


Figure 5. Molecular adsorption structure of (a) silica/PAO4, (b) silica/IL, and (c) silica/OFM interfaces. The schematics shown in (a,b) are reproduced with permission from Ref. [11], Copyright © 2020 American Chemical Society.

The *SSP* spectrum of OFM has a very weak signal at $\sim 2850\text{ cm}^{-1}$ (this peak was not captured well in the spectral fitting) while its relative intensity at $\sim 2950\text{ cm}^{-1}$ ($\text{CH}_{2,s,\text{FR}}$ or $\text{CH}_{2,\text{as}}$ of $\text{C}-\text{CH}_2-\text{O}$) is very strong. The peak at $\sim 2950\text{ cm}^{-1}$ is dominant in the *PPP* spectrum (see Table S2 in the SI). The very weak intensity of the methylene group at 2850 cm^{-1} in both *SSP* and *PPP* spectra reveals that OFM

molecules form an adsorbed layer at the silica surface with only few gauche defects. The absence of the symmetric methyl stretch peak at $\sim 2875\text{ cm}^{-1}$ suggests that SFG signals of two opposite CH_3 groups cancel out each other, indicating the formation of a multilayer structure of OFM at the interface [44]. The peak at $\sim 2950\text{ cm}^{-1}$ in the *PPP* spectrum could then be attributed to a vibrational mode of CH_2 in $\text{O-CH}_2\text{-C(OH)}$ of the head groups. The presence of a peak at $\sim 2965\text{ cm}^{-1}$ ($\text{CH}_{3,\text{as}}$) with a relatively small amplitude (see Table S2) indicates some imperfection in dipole cancelation of CH_3 groups. The polar head groups of OFM must be attached to the silica surface containing polar functional groups such as Si-OH and Si-O-Si [4,45]. The hydrogen bonds between adsorbed head groups and van der Waals forces between long alkyl chains help the formation of a well ordered layer at silica/liquid interface [4]. This also explains the strong signals of methylene groups ($\text{O-CH}_2\text{-C(OH)}$) in both *SSP* and *PPP* spectra of OFM at the silica surface. The adsorption of OFM molecules at the silica/liquid interface is schematically illustrated in Figure 5c. The thickness and order of an adsorbed layer of OFM at solid surfaces have been shown to be dependent on the molecular structure and its concentration in the lubricant [41,46].

The *SSP* and *PPP* spectra of sec-ZDDP in Figure 4 shows dominant peaks at $\sim 2940\text{ cm}^{-1}$ and weak peaks at $\sim 2870\text{ cm}^{-1}$ (see Tables S1 and S2 in the SI), while the SFG signal at $\sim 2850\text{ cm}^{-1}$ is not observed. The absence of SFG signal at $\sim 2850\text{ cm}^{-1}$ means that the $\text{-C-CH}_2\text{-C-}$ groups in the alkyl chains of sec-ZDDP at the silica surface lie in a centrosymmetric medium, so that they are SFG inactive [13]. The weak peak at $\sim 2870\text{ cm}^{-1}$ can be attributed to symmetric methylene stretch mode in $\text{O-CH}_2\text{-C}$ and/or symmetric methyl stretch mode ($\text{CH}_{3,\text{s}}$), and the dominant peak at $\sim 2940\text{ cm}^{-1}$ can be assigned to asymmetric methylene stretch mode in $\text{O-CH}_2\text{-C}$ and/or symmetric methyl Fermi resonance ($\text{CH}_{3,\text{s,FR}}$, see Table 2). Note that sec-ZDDP contains 5–10 wt.% of a mineral oil with an unknown structure and its competitive adsorption at the silica surface cannot be ruled out. Nonetheless, it can be said, based on the good SFG signal intensity, that the mixture of sec-ZDDP and mineral oil forms a well-ordered layer at the silica surface. The dominance of the SFG peaks attributable to $\text{O-CH}_2\text{-C}$ groups suggests that polar phosphate groups are likely to face toward the silica surface.

3.3. Speciation of Silica/Lubricant Interface for PAO4 Containing Single Additive

The SFG spectra of the silica/(PAO4 + one additive) interface were measured and displayed in Figure 6. The spectra of PAO4 and its mixtures with two ionic liquids at the silica surface are adapted from Ref. [11] and are given in Figure 6 for comparison. Results from the previous study showed that [N888H][DEHP] and [P8888][DEHP] were dominant at the interface between silica and (PAO4 + IL) mixtures. The preferential adsorption of ILs at the solid/lubricant interface explains the beneficial effect of the addition of a small amount of ILs in lubrication performance [19,47–49]. As in the case of silica/IL interface, the polar head groups of IL are in contact with the polar solid surface containing Si-OH and Si-O-Si groups while their alkyl chains face to the bulk liquid. The structure of the adsorbed surface layer at silica/(PAO4 + IL) interface, however, is slightly different from that of silica/IL interface [11].

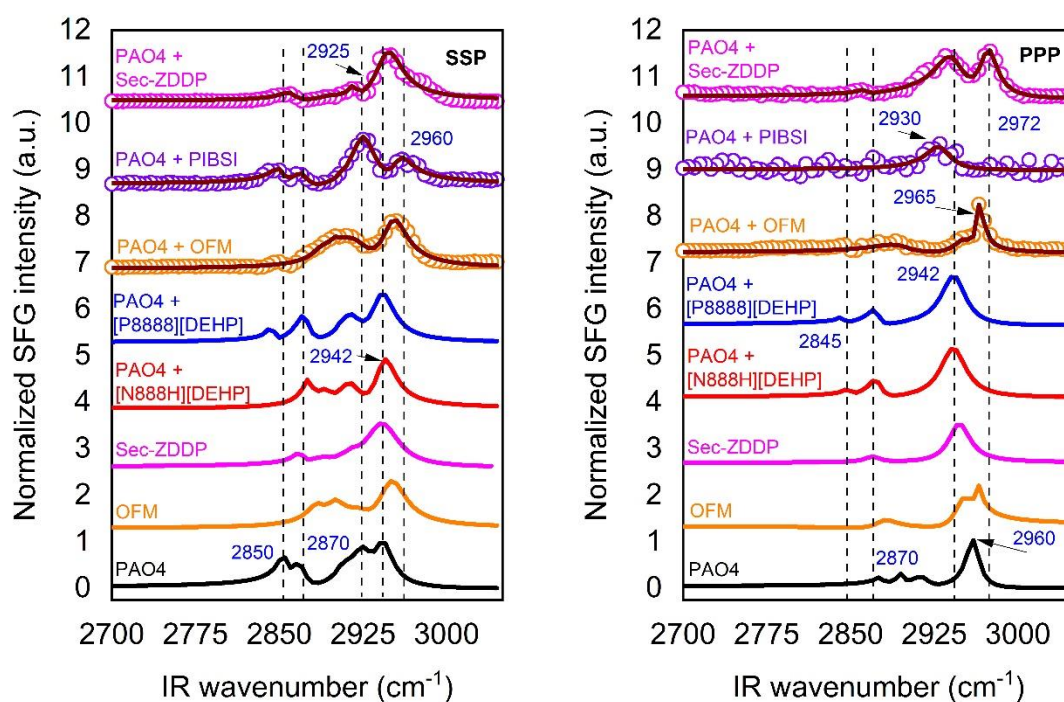


Figure 6. SFG spectra of two compound mixtures at silica/liquid interface. The solid lines are fitted curves and the fitting results are given in the SI. The line spectra of PAO4, (PAO4 + [N888H][DEHP]), and (PAO4 + [P8888][DEHP]) are adapted from Ref. [11] and shown here for comparison. The line spectra of OFM and Sec-ZDDP are replotted in Figure 6 to compare with their spectra in PAO4.

3.3.1. PAO4 + OFM Mixture

The *SSP* and *PPP* spectra of the silica/(PAO4 + OFM) interface are very similar to those of silica/OFM interface (see Figure 4 and Tables S1–S4 in the SI). It means that OFM molecules preferentially adsorb from its mixture with PAO4 to the silica surface and form a well-packed surface layer. Although the OFM concentration is much smaller than that of PAO4 in the bulk mixture (Table 1), its surface concentration at the silica interface is dominant due to the strong interaction between OFM polar head groups and the polar solid surface, as well as the van der Waals interactions between long alkyl chains of OFM molecules [4]. The similarity between SFG spectra of silica/OFM and silica/(PAO4 + OFM) interfaces also indicates that for the OFM concentration used in the current study, a multilayer structure of OFM is formed at the interface. The conformation of the OFM layer at the silica/(PAO4 + OFM) interface would be similar to the one illustrated in Figure 5c except that the bulk liquid is now a mixture of PAO4 and OFM. The formation of a surface layer by the preferential adsorption of OFM from its mixture with the lubricant base oil is consistent with results reported in the literature [41,46]. The adsorbed surface layer greatly reduced the interfacial friction in tribological operation conditions [41].

3.3.2. PAO4 + PIBSI Mixture

The *SSP* spectrum of this mixture at the silica surface is significantly different from that of PAO4. It has a peak at 2956 cm^{-1} that is not observed in the spectrum of PAO4. The *SSP* spectrum of this mixture is very similar to that of silica/hexadecane interface [11]. The strong peak at $\sim 2925\text{ cm}^{-1}$ in the *SSP* spectrum is assigned to symmetric methylene Fermi resonance of C–CH₂–C (see Table 2) and the only peak at $\sim 2930\text{ cm}^{-1}$ in the *PPP* spectrum could be assigned to asymmetric methylene stretch mode (see Table 2). These results suggest that PIBSI molecules lie flat at the silica surface with the symmetry axis of CH₂ in C–CH₂–C groups aligns relatively along the surface normal (see Figure 2b, the CH₃ group can be replaced by the CH₂ group with a C₂ axis). If the peak at 2956 cm^{-1} in the *SSP* spectrum is of asymmetric methyl stretch mode (CH_{3,as}), there should be a strong peak of this

vibrational mode in the *PPP* spectrum [30]. The absence of $\sim 2956\text{ cm}^{-1}$ peak in the *PPP* spectrum then suggests that the peak is not due to asymmetric methyl stretch mode. It could, however, be attributed to symmetric methylene Fermi resonance of $\text{N-CH}_2\text{-CH}_2\text{-N}$ (see Figure 1) as in the case of 1,3-propanediol ($\text{HOCH}_2\text{CH}_2\text{CH}_2\text{OH}$) [29]. Although we cannot rule out a small fraction of PAO4 is co-adsorbed at the solid surface, the dominance of PIBSI at the solid/(PAO4 + PIBSI) interface explains the improved tribological performance of this mixture compared to the base oil only case [10,50].

3.3.3. PAO4 + sec-ZDDP Mixture

The *SSP* spectrum of the silica/(PAO4 + sec-ZDDP) interface is quite similar to that of silica/sec-ZDDP interface; however, their *PPP* spectra are different with an additional peak in the spectrum of silica/mixture interface at $\sim 2972\text{ cm}^{-1}$ which can be assigned to out-of-plane asymmetric methyl stretch mode (see Table 2). These results suggest that a mixed film of PAO4, sec-ZDDP, and mineral oil could form at the silica surface with a possible dominance of components from sec-ZDDP. The abundance of sec-ZDDP in the interfacial layer is the main reason that it works effectively as the antiwear additive even at such a low concentration in the bulk liquid [51,52].

3.4. Speciation of Silica/Lubricant Interface for PAO4 Containing Two Additives

Commercial lubricants contain multiple additives with different functionalities such as friction modifier, antiwear, dispersant, antioxidant, detergent [4,9]. In the current study, the competitive adsorption at the silica surface from PAO4-based lubricants containing IL and another additive (friction modifier, antiwear additive, or dispersant) was investigated using SFG spectroscopy. The compositions of mixed liquids are displayed in Table 1. The fitting results of the SFG spectra are available in the SI.

3.4.1. Mixtures of PAO4 + OFM + IL

The SFG spectra of silica / (PAO4 + OFM + IL) mixtures are given in Figure 7. The spectra of PAO4 and other mixtures are also displayed in Figure 7 for comparison. The *SSP* spectrum of (PAO4 + OFM + [N888H][DEHP]) mixture in Figure 7 is very similar to that of silica/(PAO4 + OFM) interface; however, their *PPP* spectra are slightly different. These results reveal that at the interface between silica and (PAO4 + OFM + [N888H][DEHP]) mixture, OFM is dominant over other two compounds and there could be a small contribution of [N888H][DEHP] to the surface layer. Results from a previous study showed a strong synergistic effect between OFM and [N888H][DEHP]; the tribological test with bronze and the lubricant containing both OFM and [N888H][DEHP] resulted in a significantly lower steady-state friction coefficient and wear rate compared to the test with the lubricant containing OFM or [N888H][DEHP] alone [9]. The outstanding lubrication performance of (OFM + [N888H][DEHP]) mixture was attributed to a physically adsorbed mixed surface film providing the benefits of both additives and the formation of such a film is enhanced by possible hydrogen bonds between OFM and [N888H][DEHP] at the bronze surface [9]. The slight difference in *PPP* spectra of silica/(PAO4 + OFM) and silica/(PAO4 + OFM + [N888H][DEHP]) could confirm the formation of such mixed film at the silica surface (and the oxide layer on bronze as well [9]). The interface between silica and (PAO4 + OFM + [N888H][DEHP]) mixture is schematically illustrated in Figure 8a.

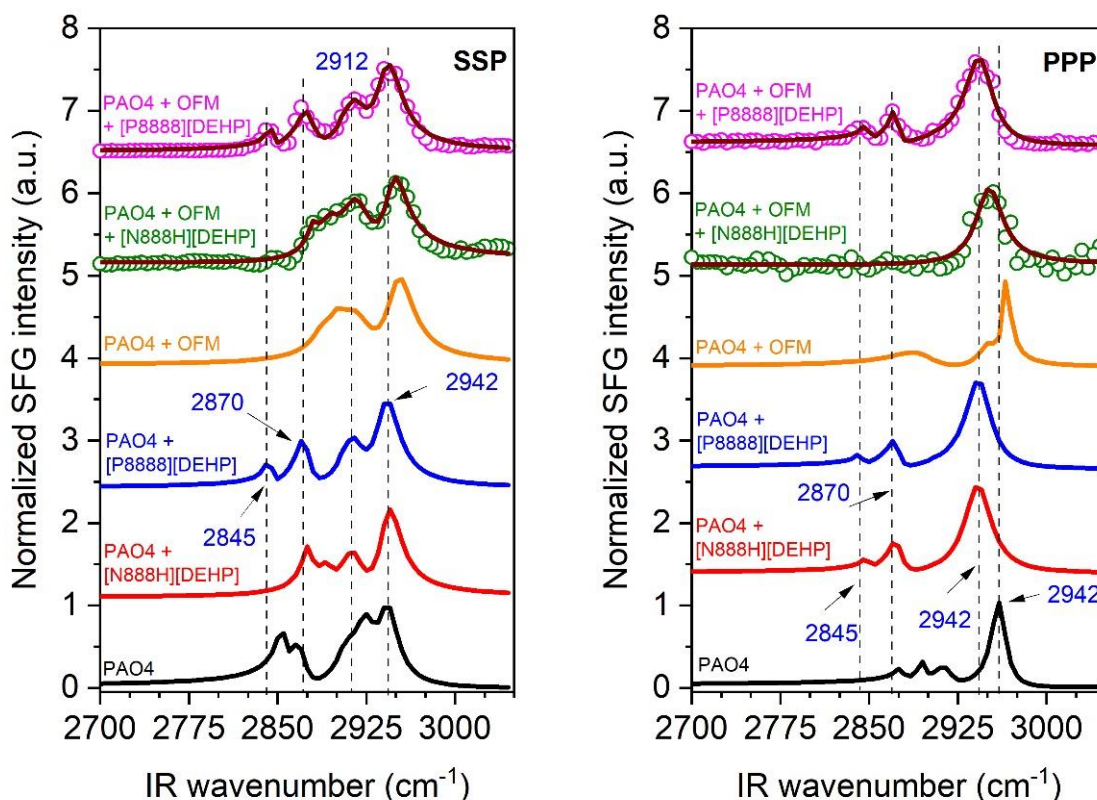


Figure 7. SFG spectra of (PAO4 + OFM + IL) mixtures at silica/liquid interface. The solid lines are fitted curves and the fitting results are given in the SI. The line spectra of PAO4, PAO4 + [N888H][DEHP], PAO4 + [P8888][DEHP] are adapted from Ref. [11] and shown here for comparison.

The *SSP* and *PPP* spectra of silica/(PAO4 + OFM + [P8888][DEHP]) interface in Figure 7 are very similar to those of silica/(PAO4 + [P8888][DEHP]) interface (see Tables S3–S6). Both *SSP* spectra have the same peaks at ~ 2850 cm^{-1} , 2870 cm^{-1} , 2915 cm^{-1} and 2940 cm^{-1} (see Table 2 for possible spectral assignments) and their *PPP* spectra contain peaks at ~ 2850 cm^{-1} , 2870 cm^{-1} , and 2940 cm^{-1} . These results show that [P8888][DEHP] preferentially adsorbs to the silica surface from the mixture of these three compounds [11]. The polar head groups of [P8888][DEHP] molecules must be in contact with the silica, while their alkyl chains face to the bulk liquid (see Figure 8b). In the tribological study at the bronze surface, the adsorption of OFM to the solid surface from its mixture with PAO4 and [P8888][DEHP] was considered to be affected by strong intermolecular hydrogen bonds between OFM and [P8888][DEHP] in the liquid phase, in addition to inevitable competitive adsorption between these two compounds [9]. However, these hydrogen bonds could also affect the adsorption of [P8888][DEHP] at the bronze surface. The SFG results in this study suggest that the presence of one more alkyl chain in [P8888]⁺ compared to [N888H]⁺ can cause drastic differences in the adsorption of these ILs to the silica surface from their mixtures with PAO4 and OFM.

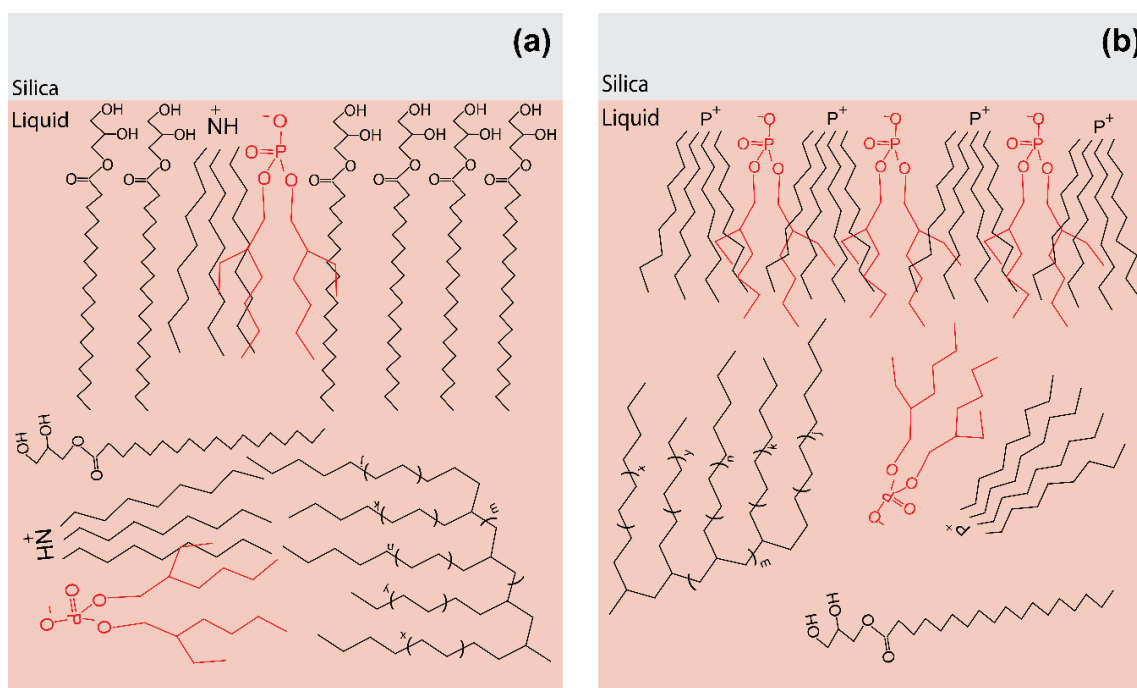


Figure 8. (a) Illustration of silica/(PAO4 + OFM + [N888H][DEHP]) interface and (b) that of silica/(PAO4 + OFM + [P8888][DEHP]) interface.

3.4.2. Mixtures of PAO4 + sec-ZDDP + IL

The *SSP* and *PPP* spectra of the silica/(PAO4 + sec-ZDDP + IL) interface are shown in Figure 9. These spectra are very similar to those of the silica/(PAO4 + IL) interface (see Tables S3–S6 in the SI). Note that the *PPP* spectra of the silica/(PAO4 + sec-ZDDP + IL) interface do not show a peak at $\sim 2845\text{ cm}^{-1}$ and the absence of this peak could be due to a low S/N ratio. The results in Figure 9 reveal that the silica surface is dominated by IL molecules even though its concentration in the bulk liquid is very low. Both ionic liquids containing polar head groups have stronger interactions with the silica surface compared to other components in the mixtures leading to their preferential adsorption at the interface.

Synergistic effects between sec-ZDDP and [P8888][DEHP] in tribological experiments were reported in the literature [6], in which the presence of these compounds together in the lubricant lead to $\sim 30\%$ reduction in friction and $\sim 70\%$ reduction in wear compared to lubricants containing base oil + sec-ZDDP (or [P8888][DEHP]) only. The fact that SFG spectra of silica/(PAO4 + [P8888][DEHP]) and silica/(PAO4 + sec-ZDDP + [P8888][DEHP]) interfaces are very similar indicates that the reductions in friction and wear in the case of PAO4 + sec-ZDDP + [P8888][DEHP] mixture could be related to the properties of the tribofilm formed during the tribological test, rather than the initial surface film before tribo-test. It was shown that this tribofilm, compared to the tribofilms formed with the lubricants containing sec-ZDDP or [P8888][DEHP] only, has significantly higher amounts of zinc and iron phosphates while having much lower contents of metal oxides and sulfur compounds [6]. The previous study also suggested that both cations and anions of IL have critical roles in reductions of friction and wear. This also explains why [N888H][DEHP] did not show synergistic effects with sec-ZDDP [6] although it dominates the solid surface before the onset of the tribo-test (as shown in Figure 9, assuming that adsorptions of base oil and additives at the silica and metal oxide surfaces are similar).

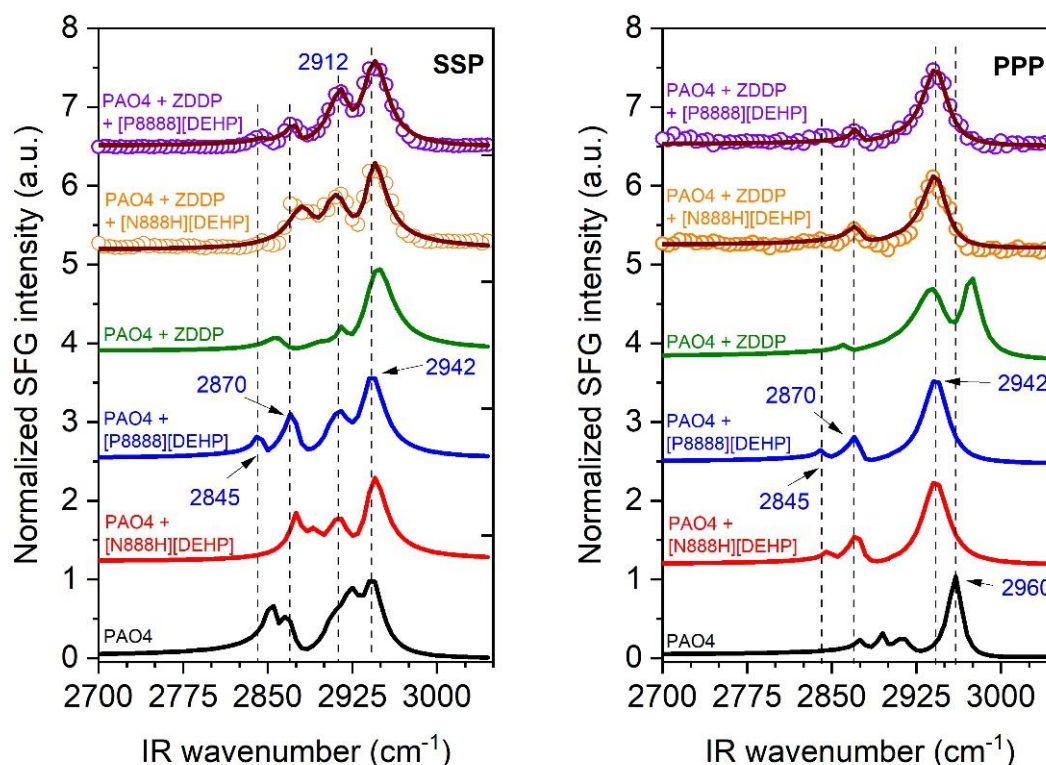


Figure 9. SFG spectra of (PAO4 + ZDDP + IL) mixtures at silica/liquid interface. The solid lines are fitted curves and the fitting results are given in the SI. The line spectra of PAO4, PAO4 + [N888H][DEHP], PAO4 + [P888H][DEHP] are adapted from Ref. [11] and shown here for comparison.

3.4.3. Mixtures of PAO4 + PIBSI + IL

The SFG spectra of the silica/(PAO4 + PIBSI + IL) interface are shown in Figure 10 along with the spectra of other mixtures for comparison. The *SSP* spectrum of the (PAO4 + PIBSI + [N888H][DEHP]) mixture is quite similar to that of the (PAO4 + PIBSI) mixture, while its *PPP* spectrum is similar to the spectrum of the (PAO4 + [N888H][DEHP]) mixture (see Tables S3–S6). This means that at the interface between silica and the (PAO4 + PIBSI + [N888H][DEHP]) mixture, PIBSI and [N888H] co-adsorb to form a mixed layer with an insignificant contribution from PAO4. Tribological tests on a cast iron surface showed that the friction coefficient and wear volume of cast iron were higher when tested with the (PAO4 + PIBSI + [N888H][DEHP]) mixture compared to those in the case of testing with the (PAO4 + [N888H][DEHP]) mixture [10]. These higher values could be due to a reduced amount of [N888H][DEHP] at the solid surface when used together with PIBSI in the lubricant as evidenced by SFG results in the current study.

The *SSP* spectrum of (PAO4 + PIBSI + [P888H][DEHP]) mixture at the silica surface is quite similar to that of (PAO4 + PIBSI) and their *PPP* spectra are also quite similar (except a small peak at 2942 cm^{-1}) in terms of spectral features (see Tables S3–S6). These results suggest that at the interface between silica and three compound mixture, PIBSI molecules possibly dominate the surface layer. The absence of [P888H][DEHP] at the silica surface could be due to its reaction/interaction with PIBSI in the bulk liquid [10]. For this reason, [P888H][DEHP] may stay in the liquid phase while PIBSI preferentially adsorbs to the silica surface. The depletion of [P888H][DEHP] from the interface when used together with PIBSI can explain the results obtained in the previous study in which the (PAO4 + PIBSI + [P888H][DEHP]) mixture showed a higher friction and a more wear of cast iron compared to those of (PAO4 + [P888H][DEHP]) mixture [10].

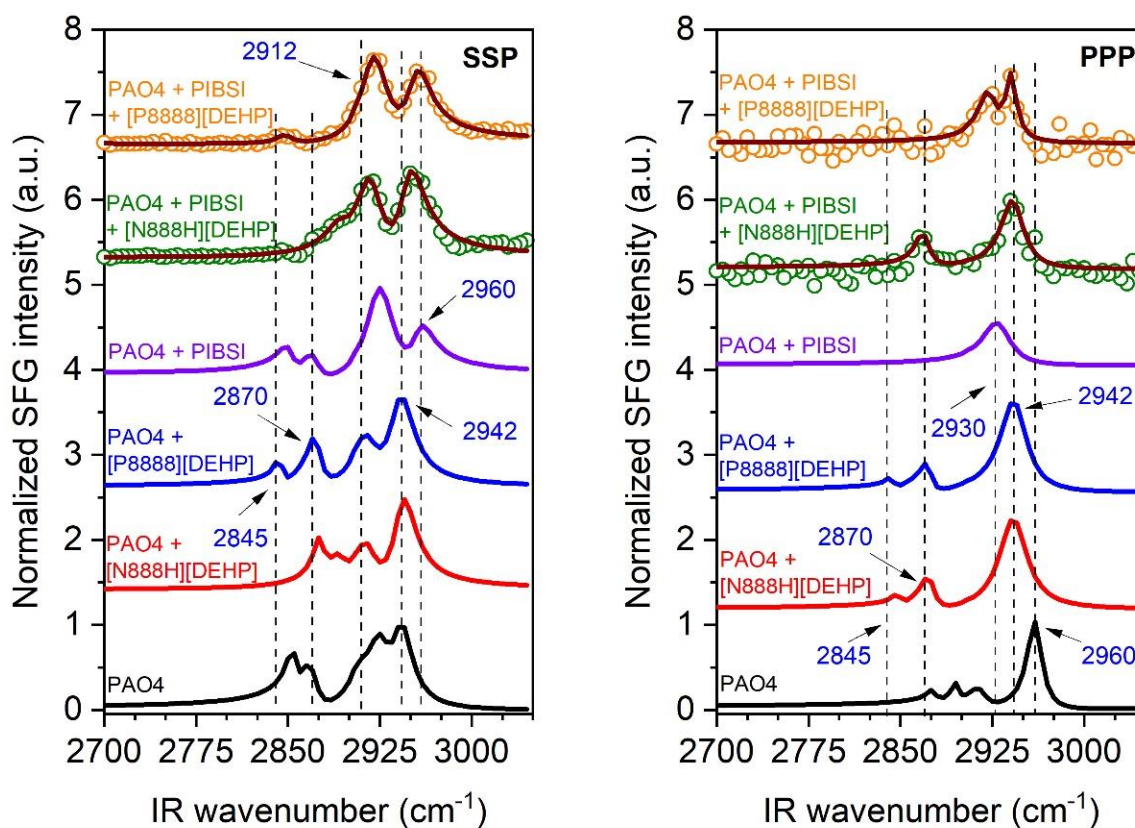


Figure 10. SFG spectra of (PAO4 + PIBSI + IL) mixtures at silica/liquid interface. The solid lines are fitted curves and the fitting results are given in the SI. The line spectra of PAO4, PAO4 + [N888H][DEHP], PAO4 + [P8888][DEHP] are adapted from Ref. [11] and shown here for comparison.

4. Conclusions

Competitive adsorption of additives at the silica/lubricant interface was studied using vibrational sum frequency generation spectroscopy. The results showed that adsorption of an additive at a solid surface can be affected by the presence of other additives in the base oil. The adsorption behavior of (base oil + additive(s)) mixtures at the silica/lubricant interface is summarized and compared with the tribological performance data found in the literature in Table 3. The correlation between adsorption behavior of additives on the silica surface and experimental results from tribological tests can provide mechanistic insights for future lubricant development, particularly important for guiding the use of ILs.

Table 3. Summary of adsorption behavior of (lubricant base oil + additive) mixtures at the silica/liquid interface and comparison with lubrication performance of the same mixtures at tribological interfaces reported in literatures.

Lubricant	Interfacial Layer	Tribological Property
PAO4 + IL	IL molecules dominate the interface [11]	Beneficial effects [9,10]
PAO4 + OFM	The interface is dominated by OFM molecules and the surface layer structure is very similar to that of silica/OFM interface.	Beneficial effects [9,41]
PAO4 + sec-ZDDP	A mixed layer of PAO4 and sec-ZDDP forms at the silica surface and sec-ZDDP dominates this surface layer.	Beneficial effects [50]
PAO4 + PIBSI	PIBSI preferential adsorbs to the silica/liquid interface and seems to lie relatively flat at the surface.	Beneficial effects [10,50]
PAO4 + OFM + [N888H][DEHP]	A mixed layer of OFM and [N888H][DEHP] is formed at the silica surface and OFM is the major component of this mixed layer.	Synergistic effects [9]
PAO4 + OFM + [P8888][DEHP]	The surface layer is dominated by [P8888][DEHP] and its structure is similar to that formed at silica/(PAO4 + [P8888][DEHP]) interface.	Lubrication efficiency was reduced in comparison to that of (PAO4 + OFM) [9]
PAO4 + sec-ZDDP + [N888H][DEHP]	[N888H][DEHP] molecules adsorb to the silica surface to form a surface layer that is similar to that of silica/(PAO4 + [N888H][DEHP]) interface.	No synergistic effect due to the presence of [N888H] ⁺ [6] (In Ref. [6] the base oil was gas-to-liquid (GTL))
PAO4 + sec-ZDDP + [P8888][DEHP]	The surface layer is dominated by [P8888][DEHP] and its structure is very similar to that of silica/(PAO4 + [P8888][DEHP]) interface.	Reduction of friction by ~30% and wear by >70% [6]. The SFG results show that this improved performance must be related to the properties of the tribofilm formed during the tribological test, rather than the initial surface film before tribo-test.
PAO4 + PIBSI + [N888H][DEHP]	PIBSI and [N888H][DEHP] form a mixed layer at the silica surface. The presence of PAO4 in the surface layer is insignificant.	Inferior performance, compared to IL only [10]
PAO4 + PIBSI + [P8888][DEHP]	PIBSI possibly dominates the silica/mixed liquid interface.	Inferior performance, compared to IL only [10]

Supplementary Materials: The following are available online at <http://www.mdpi.com/2075-4442/8/11/98/s1>, Table S1: Fitting results of SSP spectra of single compounds at solid/liquid interface, Table S2: Fitting results of PPP spectra of single compounds at solid/liquid interface, Table S3: Fitting results of SSP spectra of two compound mixtures at silica/liquid interface, Table S4: Fitting results of PPP spectra of two compound mixtures at silica/liquid interface, Table S5: Fitting results of SSP spectra of three compound mixtures at silica/liquid interface, Table S6: Fitting results of PPP spectra of three compound mixtures at the silica/liquid interface.

Author Contributions: Conceptualization, J.Q. and S.H.K.; Formal analysis, D.N.; Funding acquisition, J.Q. and S.H.K.; Investigation, D.N., X.H., H.L., J.Q. and S.H.K.; Resources, J.Q.; Supervision, S.H.K.; Writing—original draft, D.N. and S.H.K.; Writing—review and editing, D.N., X.H., H.L., J.Q. and S.H.K. All authors have read and agreed to the published version of the manuscript.

Funding: This manuscript has been co-authored by UT-Battelle, LLC under contract no. DEAC05-00OR22725 with the U.S. Department of Energy. The U.S. Government retains, and the publisher, by accepting the article for publication, acknowledges that the U.S. Government retains a nonexclusive, paid-up, irrevocable, worldwide license to publish or reproduce the published form of this manuscript, or allow others to do so, for U.S. Government purposes. The Department of Energy will provide public access to these results of federally sponsored research by the DOE public access plan (<http://energy.gov/downloads/doe-public-access-plan>).

Acknowledgments: This work was supported by the Vehicle Technologies Office, Office of Energy Efficiency and Renewable Energy, U.S. Department of Energy (DOE) as a subcontract to Pennsylvania State University through the Oak Ridge National Laboratory. The authors thank J. Dyck and E. Conrad from Solvay for providing phosphonium cation feedstocks, A.G. Bro and C. Dubin from ExxonMobil for providing the PAO base oil, O. Farnag from ExxonMobil for providing the OFM, and PIBSI, and E. Bardasz from Lubrizol for providing the ZDDP.

Conflicts of Interest: The authors declare no conflict of interest.

References

1. Seymour, B.T.; Fu, W.; Wright, R.A.E.; Luo, H.; Qu, J.; Dai, S.; Zhao, B. Improved Lubricating Performance by Combining Oil-Soluble Hairy Silica Nanoparticles and an Ionic Liquid as an Additive for a Synthetic Base Oil. *ACS Appl. Mater. Interfaces* **2018**, *10*, 15129–15139. [[CrossRef](#)]
2. Cai, M.; Guo, R.; Zhou, F.; Liu, W. Lubricating a bright future: Lubrication contribution to energy saving and low carbon emission. *Sci. China Technol. Sci.* **2013**, *56*, 2888–2913. [[CrossRef](#)]
3. Holmberg, K.; Andersson, P.; Erdemir, A. Global energy consumption due to friction in passenger cars. *Tribol. Int.* **2012**, *47*, 221–234. [[CrossRef](#)]
4. Rudnick, L.R. *Lubricant Additives: Chemistry and Applications*, 3rd ed.; CRC Press: Boca Raton, FL, USA, 2017.
5. Guegan, J.; Southby, M.; Spikes, H. Friction Modifier Additives, Synergies and Antagonisms. *Tribol. Lett.* **2019**, *67*, 83. [[CrossRef](#)]
6. Qu, J.; Barnhill, W.C.; Luo, H.; Meyer, H.M., III; Leonard, D.N.; Landauer, A.K.; Kheireddin, B.; Gao, H.; Papke, B.L.; Dai, S. Synergistic Effects Between Phosphonium-Alkylphosphate Ionic Liquids and Zinc Dialkyldithiophosphate (ZDDP) as Lubricant Additives. *Adv. Mater.* **2015**, *27*, 4767–4774. [[CrossRef](#)] [[PubMed](#)]
7. Bec, S.; Tonck, A.; Georges, J.M.; Roper, G.W. Synergistic Effects of MoDTC and ZDTP on Frictional Behaviour of Tribofilms at the Nanometer Scale. *Tribol. Lett.* **2004**, *17*, 797–809. [[CrossRef](#)]
8. Martin, J.M.; Grossiord, C.; Varlot, K.; Vacher, B.; Igarashi, J. Synergistic effects in binary systems of lubricant additives: A chemical hardness approach. *Tribol. Lett.* **2000**, *8*, 193–201. [[CrossRef](#)]
9. Li, W.; Kumara, C.; Meyer, H.M.; Luo, H.; Qu, J. Compatibility between Various Ionic Liquids and an Organic Friction Modifier as Lubricant Additives. *Langmuir* **2018**, *34*, 10711–10720. [[CrossRef](#)]
10. Li, W.; Kumara, C.; Luo, H.; Meyer, H.M.; He, X.; Ngo, D.; Kim, S.H.; Qu, J. Ultralow Boundary Lubrication Friction by Three-Way Synergistic Interactions among Ionic Liquid, Friction Modifier, and Dispersant. *ACS Appl. Mater. Interfaces* **2020**, *12*, 17077–17090. [[CrossRef](#)]
11. Ngo, D.; He, X.; Luo, H.; Qu, J.; Kim, S.H. Competitive Adsorption of Lubricant Base Oil and Ionic Liquid Additives at Air/Liquid and Solid/Liquid Interfaces. *Langmuir* **2020**, *36*, 7582–7592. [[CrossRef](#)]
12. Zhou, Y.; Qu, J. Ionic Liquids as Lubricant Additives: A Review. *ACS Appl. Mater. Interfaces* **2017**, *9*, 3209–3222. [[CrossRef](#)] [[PubMed](#)]
13. Lambert, A.G.; Davies, P.B.; Neivandt, D.J. Implementing the Theory of Sum Frequency Generation Vibrational Spectroscopy: A Tutorial Review. *Appl. Spectrosc. Rev.* **2005**, *40*, 103–145. [[CrossRef](#)]
14. Bain, C.D. Sum-frequency vibrational spectroscopy of the solid/liquid interface. *J. Chem. Soc. Faraday Trans.* **1995**, *91*, 1281–1296. [[CrossRef](#)]
15. Chae, I.; Ngo, D.; Makarem, M.; Ounaies, Z.; Kim, S.H. Compression-Induced Topographic Corrugation of Air/Surfactant/Water Interface: Effect of Nanoparticles Adsorbed beneath the Interface. *J. Phys. Chem. C* **2019**, *123*, 25628–25634. [[CrossRef](#)]
16. Romero, C.; Baldelli, S. Sum Frequency Generation Study of the Room-Temperature Ionic Liquids/Quartz Interface. *J. Phys. Chem. B* **2006**, *110*, 6213–6223. [[CrossRef](#)] [[PubMed](#)]
17. Rivera-Rubero, S.; Baldelli, S. Surface Spectroscopy of Room-temperature Ionic Liquids on a Platinum Electrode: A Sum Frequency Generation Study. *J. Phys. Chem. B* **2004**, *108*, 15133–15140. [[CrossRef](#)]
18. Baldelli, S. Interfacial Structure of Room-Temperature Ionic Liquids at the Solid–Liquid Interface as Probed by Sum Frequency Generation Spectroscopy. *J. Phys. Chem. Lett.* **2013**, *4*, 244–252. [[CrossRef](#)]
19. Barnhill, W.C.; Qu, J.; Luo, H.; Meyer, H.M.; Ma, C.; Chi, M.; Papke, B.L. Phosphonium-Organophosphate Ionic Liquids as Lubricant Additives: Effects of Cation Structure on Physicochemical and Tribological Characteristics. *ACS Appl. Mater. Interfaces* **2014**, *6*, 22585–22593. [[CrossRef](#)]

20. Elsentriecy, H.H.; Qu, J.; Luo, H.; Meyer, H.M.; Ma, C.; Chi, M. Improving corrosion resistance of AZ31B magnesium alloy via a conversion coating produced by a protic ammonium-phosphate ionic liquid. *Thin Solid Film.* **2014**, *568*, 44–51. [[CrossRef](#)]
21. Mendes Siqueira, A.L.; Beaumesnil, M.; Hubert-Roux, M.; Loutelier-Bourhis, C.; Afonso, C.; Pondaven, S.; Bai, Y.; Racaud, A. Characterization of polyalphaolefins using halogen anion attachment in atmospheric pressure photoionization coupled with ion mobility spectrometry-mass spectrometry. *Analyst* **2018**, *143*, 3934–3940. [[CrossRef](#)]
22. Snyder, R.G.; Strauss, H.L.; Elliger, C.A. Carbon-hydrogen stretching modes and the structure of n-alkyl chains. 1. Long, disordered chains. *J. Phys. Chem.* **1982**, *86*, 5145–5150. [[CrossRef](#)]
23. Snyder, R.G.; Hsu, S.L.; Krimm, S. Vibrational spectra in the C—H stretching region and the structure of the polymethylene chain. *Spectrochim. Acta Part A Mol. Spectrosc.* **1978**, *34*, 395–406. [[CrossRef](#)]
24. Esenturk, O.; Walker, R.A. Surface Structure at Hexadecane and Halo-hexadecane Liquid/Vapor Interfaces. *J. Phys. Chem. B* **2004**, *108*, 10631–10635. [[CrossRef](#)]
25. MacPhail, R.A.; Strauss, H.L.; Snyder, R.G.; Elliger, C.A. Carbon-hydrogen stretching modes and the structure of n-alkyl chains. 2. Long, all-trans chains. *J. Phys. Chem.* **1984**, *88*, 334–341. [[CrossRef](#)]
26. Walker, R.A.; Conboy, J.C.; Richmond, G.L. Molecular Structure and Ordering of Phospholipids at a Liquid–Liquid Interface. *Langmuir* **1997**, *13*, 3070–3073. [[CrossRef](#)]
27. Conboy, J.C.; Messmer, M.C.; Richmond, G.L. Dependence of Alkyl Chain Conformation of Simple Ionic Surfactants on Head Group Functionality As Studied by Vibrational Sum-Frequency Spectroscopy. *J. Phys. Chem. B* **1997**, *101*, 6724–6733. [[CrossRef](#)]
28. Tyrode, E.; Hedberg, J. A Comparative Study of the CD and CH Stretching Spectral Regions of Typical Surfactants Systems Using VSFS: Orientation Analysis of the Terminal CH₃ and CD₃ Groups. *J. Phys. Chem. C* **2012**, *116*, 1080–1091. [[CrossRef](#)]
29. Lu, R.; Gan, W.; Wu, B.-H.; Chen, H.; Wang, H.-F. Vibrational Polarization Spectroscopy of CH Stretching Modes of the Methylene Group at the Vapor/Liquid Interfaces with Sum Frequency Generation. *J. Phys. Chem. B* **2004**, *108*, 7297–7306. [[CrossRef](#)]
30. Wang, H.-F.; Gan, W.; Lu, R.; Rao, Y.; Wu, B.-H. Quantitative spectral and orientational analysis in surface sum frequency generation vibrational spectroscopy (SFG-VS). *Int. Rev. Phys. Chem.* **2005**, *24*, 191–256. [[CrossRef](#)]
31. Peñalber-Johnstone, C.; Adamová, G.; Plechkova, N.V.; Bahrami, M.; Ghaed-Sharaf, T.; Ghatee, M.H.; Seddon, K.R.; Baldelli, S. Sum frequency generation spectroscopy of tetraalkylphosphonium ionic liquids at the air–liquid interface. *J. Chem. Phys.* **2018**, *148*, 193841. [[CrossRef](#)]
32. Bell, G.R.; Manning-Benson, S.; Bain, C.D. Effect of Chain Length on the Structure of Monolayers of Alkyltrimethylammonium Bromides (CnTABs) at the Air–Water Interface. *J. Phys. Chem. B* **1998**, *102*, 218–222. [[CrossRef](#)]
33. Walker, R.A.; Gruetzmacher, J.A.; Richmond, G.L. Phosphatidylcholine Monolayer Structure at a Liquid–Liquid Interface. *J. Am. Chem. Soc.* **1998**, *120*, 6991–7003. [[CrossRef](#)]
34. Bain, C.D.; Davies, P.B.; Ong, T.H.; Ward, R.N.; Brown, M.A. Quantitative analysis of monolayer composition by sum-frequency vibrational spectroscopy. *Langmuir* **1991**, *7*, 1563–1566. [[CrossRef](#)]
35. Dreesen, L.; Humbert, C.; Hollander, P.; Mani, A.A.; Ataka, K.; Thiry, P.A.; Peremans, A. Study of the water/poly(ethylene glycol) interface by IR-visible sum-frequency generation spectroscopy. *Chem. Phys. Lett.* **2001**, *333*, 327–331. [[CrossRef](#)]
36. Hommel, E.L.; Merle, J.K.; Ma, G.; Hadad, C.M.; Allen, H.C. Spectroscopic and Computational Studies of Aqueous Ethylene Glycol Solution Surfaces. *J. Phys. Chem. B* **2005**, *109*, 811–818. [[CrossRef](#)]
37. Matsuura, H.; Miyazawa, T. Infrared spectra and molecular vibrations of ethylene glycol and deuterated derivatives. *Bull. Chem. Soc. Jpn.* **1967**, *40*, 85–94. [[CrossRef](#)]
38. Koshima, H.; Kamano, H.; Hisaeda, Y.; Liu, H.; Ye, S. Analyses of the Adsorption Structures of Friction Modifiers by Means of Quantitative Structure-Property Relationship Method and Sum Frequency Generation Spectroscopy. *Tribol. Online* **2010**, *5*, 165–172. [[CrossRef](#)]
39. Koshima, H.; Iyotani, Y.; Peng, Q.; Ye, S. Study of Friction-Reduction Properties of Fatty Acids and Adsorption Structures of their Langmuir-Blodgett Monolayers using Sum-Frequency Generation Spectroscopy and Atomic Force Microscopy. *Tribol. Lett.* **2016**, *64*, 34. [[CrossRef](#)]

40. Watanabe, S.; Nakano, M.; Miyake, K.; Sasaki, S. Analysis of the Interfacial Molecular Behavior of a Lubrication Film of n-Dodecane Containing Stearic Acid under Lubricating Conditions by Sum Frequency Generation Spectroscopy. *Langmuir* **2016**, *32*, 13649–13656. [[CrossRef](#)]
41. Fry, B.M.; Moody, G.; Spikes, H.A.; Wong, J.S.S. Adsorption of Organic Friction Modifier Additives. *Langmuir* **2020**, *36*, 1147–1155. [[CrossRef](#)]
42. Zhao, W.; Zhao, X.; Rafailovich, M.H.; Sokolov, J.; Composto, R.J.; Smith, S.D.; Russell, T.P.; Dozier, W.D.; Mansfield, T.; Satkowski, M. Segregation of chain ends to polymer melt surfaces and interfaces. *Macromolecules* **1993**, *26*, 561–562. [[CrossRef](#)]
43. Stein, G.E.; Laws, T.S.; Verduzco, R. Tailoring the Attraction of Polymers toward Surfaces. *Macromolecules* **2019**, *52*, 4787–4802. [[CrossRef](#)]
44. Liu, J.; Conboy, J.C. Direct Measurement of the Transbilayer Movement of Phospholipids by Sum-Frequency Vibrational Spectroscopy. *J. Am. Chem. Soc.* **2004**, *126*, 8376–8377. [[CrossRef](#)] [[PubMed](#)]
45. Spikes, H. Friction Modifier Additives. *Tribol. Lett.* **2015**, *60*, 5. [[CrossRef](#)]
46. Wood, M.H.; Casford, M.T.; Steitz, R.; Zarbakhsh, A.; Welbourn, R.J.L.; Clarke, S.M. Comparative Adsorption of Saturated and Unsaturated Fatty Acids at the Iron Oxide/Oil Interface. *Langmuir* **2016**, *32*, 534–540. [[CrossRef](#)]
47. Qu, J.; Bansal, D.G.; Yu, B.; Howe, J.Y.; Luo, H.; Dai, S.; Li, H.; Blau, P.J.; Bunting, B.G.; Mordukhovich, G.; et al. Antiwear Performance and Mechanism of an Oil-Miscible Ionic Liquid as a Lubricant Additive. *ACS Appl. Mater. Interfaces* **2012**, *4*, 997–1002. [[CrossRef](#)]
48. Yu, B.; Bansal, D.G.; Qu, J.; Sun, X.; Luo, H.; Dai, S.; Blau, P.J.; Bunting, B.G.; Mordukhovich, G.; Smolenski, D.J. Oil-miscible and non-corrosive phosphonium-based ionic liquids as candidate lubricant additives. *Wear* **2012**, *289*, 58–64. [[CrossRef](#)]
49. Barnhill, W.C.; Luo, H.; Meyer, H.M.; Ma, C.; Chi, M.; Papke, B.L.; Qu, J. Tertiary and Quaternary Ammonium-Phosphate Ionic Liquids as Lubricant Additives. *Tribol. Lett.* **2016**, *63*, 22. [[CrossRef](#)]
50. Wright, R.A.; Wang, K.; Qu, J.; Zhao, B. Oil-soluble polymer brush grafted nanoparticles as effective lubricant additives for friction and wear reduction. *Angew. Chem.* **2016**, *128*, 8798–8802. [[CrossRef](#)]
51. Spikes, H. The History and Mechanisms of ZDDP. *Tribol. Lett.* **2004**, *17*, 469–489. [[CrossRef](#)]
52. Zhang, J.; Ewen, J.P.; Ueda, M.; Wong, J.S.S.; Spikes, H.A. Mechanochemistry of Zinc Dialkyldithiophosphate on Steel Surfaces under Elastohydrodynamic Lubrication Conditions. *ACS Appl. Mater. Interfaces* **2020**, *12*, 6662–6676. [[CrossRef](#)] [[PubMed](#)]

Publisher's Note: MDPI stays neutral with regard to jurisdictional claims in published maps and institutional affiliations.



© 2020 by the authors. Licensee MDPI, Basel, Switzerland. This article is an open access article distributed under the terms and conditions of the Creative Commons Attribution (CC BY) license (<http://creativecommons.org/licenses/by/4.0/>).